Refractive Index, Band Gap and Oscillator Parameters of ZnO: (P-Naphtholbenzenin(α)) Flims

[1]Fadhil A. Tuma
[1] Physics Department, College of Education for Pure Sciences, of University
Basrah, Basrah, Iraq
e.mail: ghufranmsh@yahoo.com

[2]Ghufran M. Shabeeb,
[2] Department of Material Sciences, Polymer Research Center, University of Basra,

[2]Haider Abdulelah
[2] Department of Material Sciences, Polymer Research Center, University of Basra,

ABSTRACT

A semiconductor ZnO with a broad band gap, cheap cost, and flexibility that can be employed in a wide range of technical and scientific applications. In order to investigate the optical quality of ZnO, the paper explains how to manufacture it utilizing a sol-gel procedure with ((P- Naphtholbenzein(α)) dye. ZnO films' optical and structural characteristics were examined. Scientists used X-ray diffraction to characterize the unique ZnO:dye (XRD). Optical and dispersion parameters were determined by measuring transmittance in the wavelength range (300-900nm).
The optical band gap of ZnO thin films obtained via the sol–gel approach was (3.04 eV), while the optical band gap of ZnO:dye thin films was (2.95 eV).

Keywords: Zinc oxide/ dye; crystallite size; optical band gap; Oscillator Parameters

Introduction

Zinc oxide ZnO, which is employed in a range of applications, has recently been the subject of numerous investigations. To increase the chemical stability of photo anodes and the ratio of surface to volume in solar cells, Qiang Zhang et al. used ZnO nanorods to make dye-sensitized solar cells [1].

In many kinds of solar cells, zinc oxide (ZnO) has been widely studied[2-4]. Because it has a comparable band gap and electron injection process from excited dye molecules as TiO_2, ZnO has gained a lot of attention as a DSSCs alternative photo anode material[5,6]. In addition, electron mobility in ZnO is high (200 1000 cm2/(V.S))[7]. However, due to its low chemical stability in acidic dye solutions and the DSSCs electrolyte solution, ZnO's application as a photo anode material in DSSCS has been limited [8]. Defects are simply formed in ZnO, producing electron-hole reinstallation at the interface and enhancing the Zn^{2+}/dye complex [9-12]. One option for addressing the disadvantages of ZnO-based photo anodes is to coat the surface of the as-deposited ZnO with a chemically stable shell. This core-shell arrangement will passivity the surface of Zn, decreasing the compound and establishing an roadblock, which will reduce electron-hole [13]. The biomimetization of eggshell membranes to produce metallic oxide powders with pyramidal structures constructed by nanocrystals is a blain process able to manufacturing metallic oxide powders with nanocrystal-based pyramidal structures[14]. TiO_2 and ZnO have been investigated

extensively for application in dye-sensitized solar cells (DSSCs). These materials are promising for application in DSSCs because they can be made with features including large surface area, light-absorbing crystallographic flaws, and small crystallite size[15].

Nanostructure TiO_2 has been considered the most efficient material for DSSCs, although many studies have revealed ZnO as the best one than TiO_2 substitute due to its high electron mobility [16]. Semiconductors' electron conduction capacity and light absorption are affected by crystallographic defects . Interface defects and mass defects in TiO_2 electrolyte are among the things that obstruct electron transfer and cause unwanted recombination [17]. Nonradioactive defects are detrimental to the photovoltaic output of ZnO DSSCs when used at high concentrations, according to various studies in ZnO DSSCs applications, while samples with green photo luminescent emission for radioactive defects are no better than samples with orang-red photo luminescent emission[18]. The shape of the molecules is one of the most important aspects of operating DSSCs in semiconductors. Because one-dimensional structures such as fibers, tubes, and wires provide a large surface area for dye adsorption, there has recently been a lot of interest in using them to make optical layers in DSSCS, as well as improved electron transport and unit surface photovoltaic performance[19] .

Theopolina Amakali et al. was able to deposit ZnO thin films on a glass substrate to produce molecular metal (MPM) using two simple, low-cost techniques[20]. To modify the optical properties of ZnO thin films, several techniques have been proposed, including both chemical and physical processes. Sputtering techniques are one type of physical method [21–23]. Chemical methods can also be used to make ZnO thin films, but the traditional sol–gel method is often preferred over other chemical methods due to its easily and lower crystallization rate[24].

In the literature, structural and optical properties of ZnO thin films prepared by the

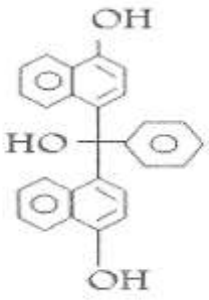

sol–gel technique with a variety of inorganic and organic precursors under various deposition conditions have been reported [25–27].

Experimental

ZnO was made using the sol-gel method, according to the handbook [28]. Zinc acetate added to the combination of isopropanol and ethanolamine. The volume of Zinc-acetate was increased to 1.0 mole. The mixture was agitated at 600°C for 1 hour ,when the solution become homogenous, then deposited it on glass substrates using the spin-coating process. A chemical approach was used to make the dye (P-Naphtholbenzenin(α)), as detailed in the handbook [29]. Figure 1 shows the molecular structure of the dye. (P-Naphtholbenzenin(α)) dye has gained a lot of attention because of its environmental resilience, ease of manufacture, and optical and electrical properties. The dye powder was dissolved in DMSO and agitated at room temperature for 3-4 hours. The ZnO thin films were heated for 1 hour at 6500°C at a rate of 500°C/min[28] in a furnace, then dipped in the dye solution for 24 hours. Before vacuum drying, allow the fluid to slowly evaporate at ambient temperature.

Fig.1. shows dye structure.

1. Results and discussion

3.1Structural properties of the ZnO and ZnO:dye thin film

The films that were formed were crystalline in nature, according to X-ray diffraction analysis. These measurements were made with a Pert Pro MPD from Philips of the Netherlands, which ran at 40 KV and 20 mA , the measurements were taken. As shown in figure. 2, XRD diffraction patterns were used to determine the shift in position of the measured diffraction peaks of ZnO and ZnO: dye.

(a)

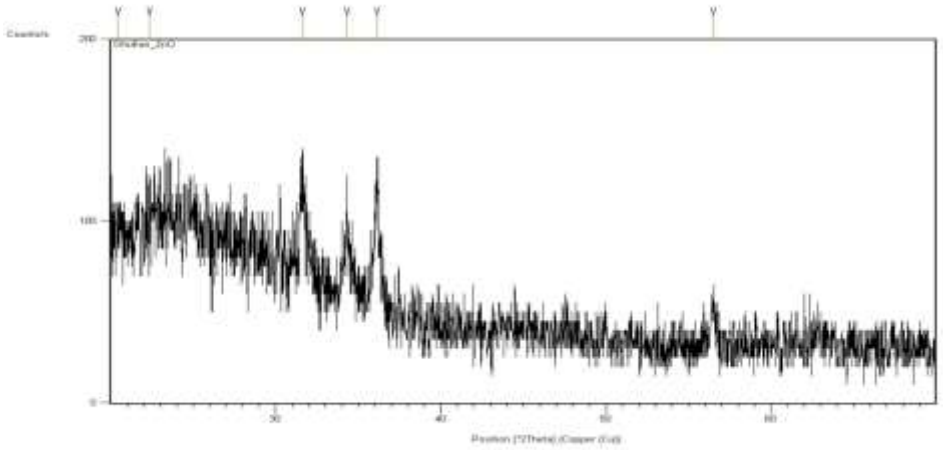

(b)

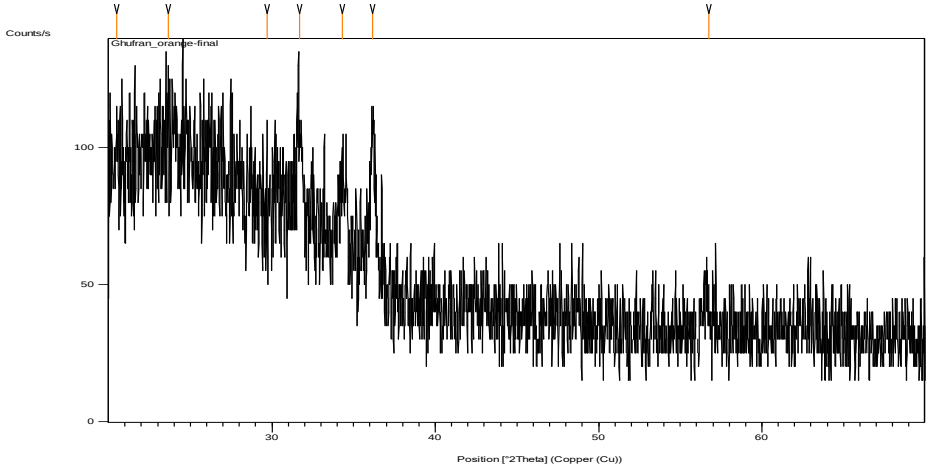

Fig. 2 . : XRD spectra of (a) ZnO, (b) ZnO:dye.

Table .1: gives the values of 2Θ , d , and I/I_0 for ZnO and ZnO:dye.

ZnO/ 2Θ[deg]	ZnO/ d[A^0]	ZnO/ I/I_0	ZnO:dye 2Θ[deg]	ZnO:dye d[A^0]	ZnO:dye I/I_0
20.4297	4.34722	70.04	23.6337	3.76463	88.42
22.3750	3.97349	100.00	29.6996	3.00811	100.00

31.6174	2.82989	91.92	31.6712	2.82521	97.55
34.3169	2.61321	65.31	34.3289	2.61232	71.72
36.1079	2.48759	93.10	36.1634	2.48391	95.17

The Debye-Scherrer formula[30] was used to calculate the grain size of the ZnO film based on XRD data.

$D = \frac{0.9\lambda}{\beta cos\theta}$ ---------- (1)

Where D is the crystallite grain size ,λ (1.5406A0) ,θ is the diffraction angle.

The grain sizes for ZnO and ZnO:dye were found to be 92 nm and 144 nm, respectively.

The absorption spectrum of ZnO and ZnO:dye is shown in figure 3.

P-Naphtholbenzenin(α) dye has an absorption spectrum that shows it can absorb visible ligh with a wavelength range of (450-550)nm and a characteristic absorption peak at 500nm.

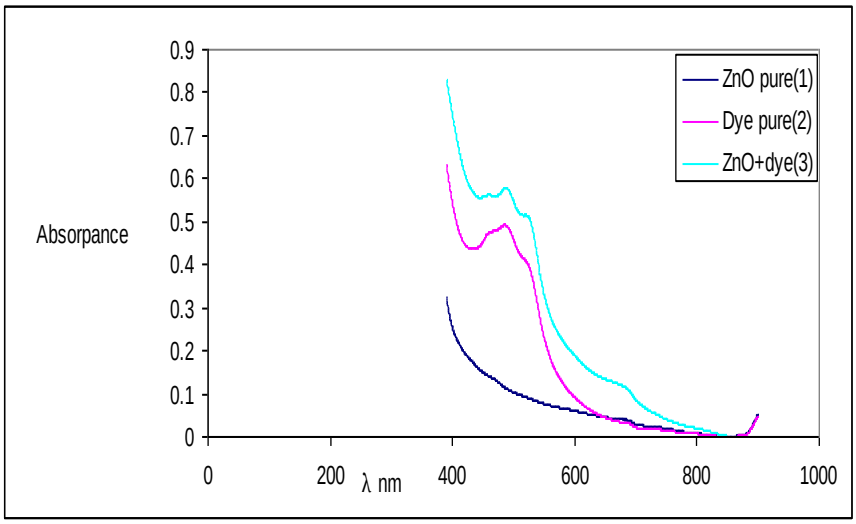

Fig.3. : Absorption spectra of ZnO, dye,ZnO:dye.

Both the refractive index (n) and the extinction coefficient (k) are used in a variety of integrated optical devices[31]. The refractive index must be changed to make it optically efficient [32]. In principle, multiple elements influence the refractive index, including the medium's polarizability and density, as well as temperature and pressure [33].

Also, in order to estimate the refractive index n of the film, the coefficient of absorption and reflection must be taken into account, as well as the absorbance[34].

$n^*(\lambda) = n(\lambda) + K(\lambda)$ -------(1)

where K denotes the extinction coefficient and n denotes the refractive index. The following is the relationship between n and k [34,35]:

$$n = \left(\frac{1+R}{1-R}\right) + \sqrt{\frac{4*R}{(1-R)^2} - K^2} \quad \text{--------(2)}$$

Where k is the extinction coefficient, which can be calculated using the relationship $K(\alpha\lambda/4\pi t)$, Where t is the thickness of the films[36,34].

R is the film's reflectance which can be calculated as[37].

$$R = \frac{(n-1)^2+k^2}{(n+1)^2+k^2} \quad \text{--------} (3)$$

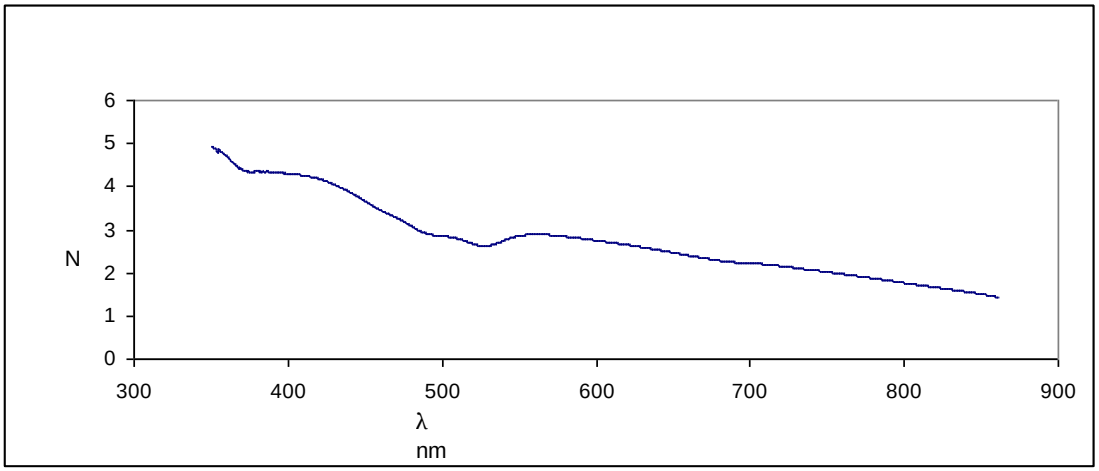

Fig.4. : The refractive index n as a function of wavelength.

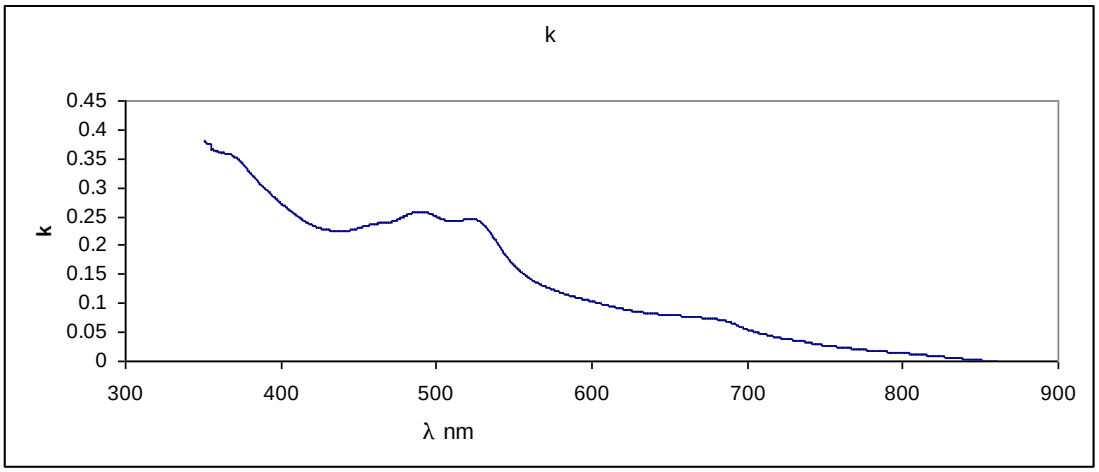

Fig.5.: The extinction coefficient k as a function of wavelength.

To make the electron transfer from the valence band to the conduction band, sufficient light energy must be absorbed, and this energy is equal to the energy gap and the relationship that shows the absorbed energy (hυ) is[42,43].

$\alpha h\upsilon = B(h\upsilon - E_g)^{\gamma}$ --------- (7)

The power coefficient is represented by the symbol. It's calculated by looking at the different types of electronic transitions that are possible, with 1/2 indicating direct allowed, 3/2 indicating direct forbidden [44,45]. The results of Tauc's model [46] are shown in Figure 6.

The thickness value is calculated using the relationship[38].

$t = \frac{M\lambda_1\lambda_2}{n_1\lambda_2 - n_2\lambda_1}$ -------- (5)

M is a one-dimensional constant.

Using the formula[39], the absorption coefficient was calculated from the spectra.

$\alpha = \frac{\ln(\frac{1}{T})}{t}$ -------- (6)

Where t is the film thickness and T is the transmittance.

Transitions from one state to another are governed by quantum mechanics' selection criteria [40,41].

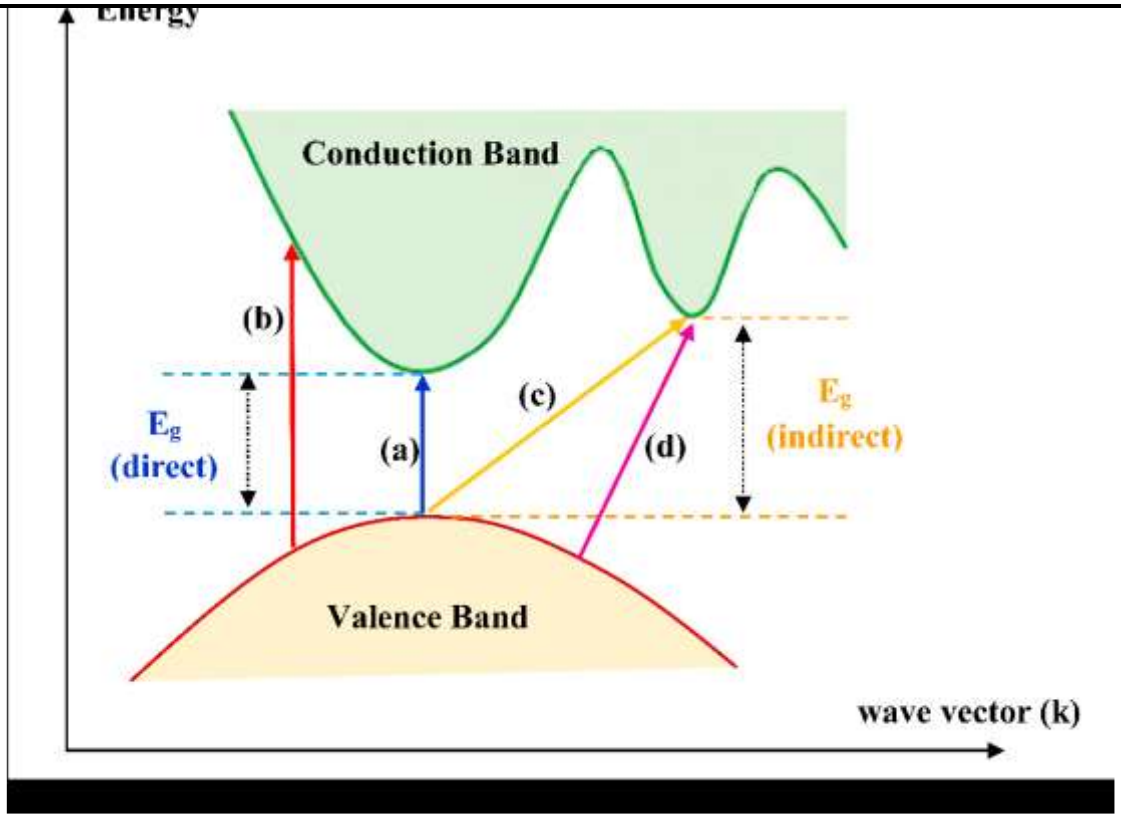

Fig. 6. : (a) direct electronic transition allowed , (b) indirect electronic transition forbidden , (c) indirect electronic transitions allowed, (d) indirect electronic transitions forbidden [47].

The free charge carriers are not absorbed and that interband transition activity is limited to high-energy photons [48].

Figure 7 shows a plot of $(\alpha h\upsilon)^2$ as a function of $h\upsilon$ to determine E_g using linear fitting.

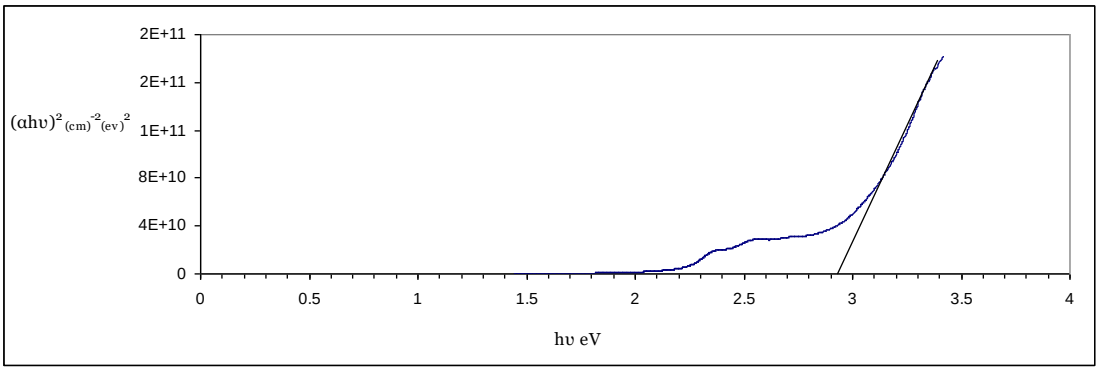

Fig. 7.: $(\alpha h\upsilon)^2$ is dependent on the photon energy $h\upsilon$.

It can written the relation for valuation the refractive index versus photon energy by using single-oscillator model by Wempel- Di Domenico[49].

$$n^2(h\nu)^{-1} = \frac{E_0 E_d}{E_0^2 - (h\nu)^2} \text{ -------- (8)}$$

Where h : plank constant, f : frequency, E_0 , E_d oscillator energy, and dispersion energy respectably.

The inverse of the equation (8):

$$(n^2-1)^{-1} = \frac{E_0^2 - (h\nu)^2}{E_0 E_d} \text{ -------- (9)}$$

Plotting $(n^2-1)^{-1}$ versus $(h\nu)^2$ as shown in figure 8 provides experimental corroboration of Equation.(9).

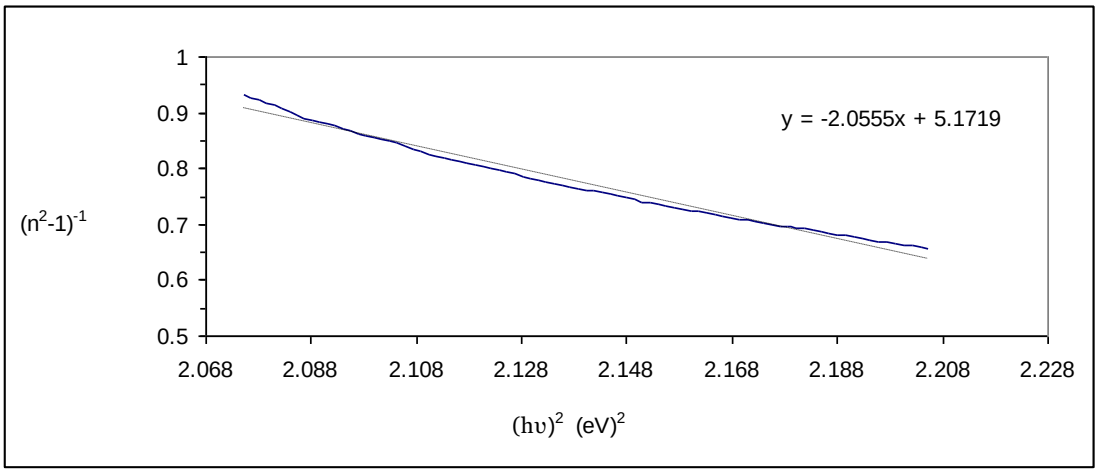

Fig.8.: Plots of $(n^2-1)^{-1}$ against $(h\nu)^2$.

As illustrated in fig.9, plotting $(n^2-1)^{-1}$ against λ^{-2} revealed that the linear component was below the absorption edge.

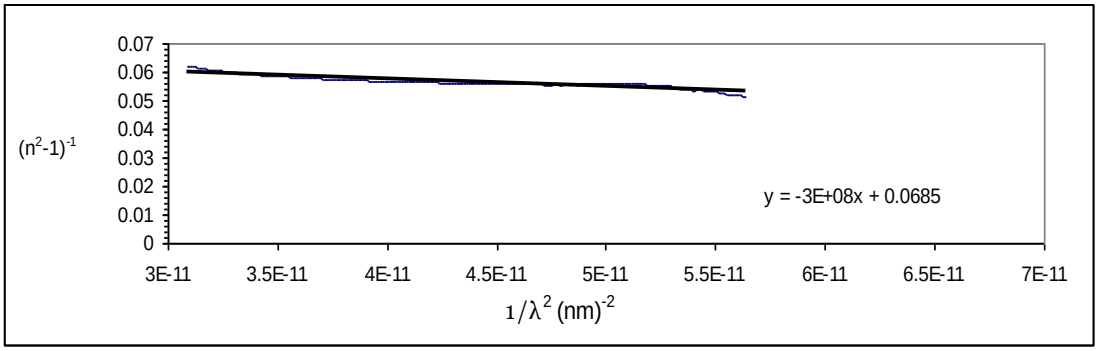

Fig. 9.: shows the graphs of $(n^2-1)^{-1}$ vs. λ^{-2}.

The approximate results of accounts of E_0,E_d, and E_g were found to be (0.66) eV,(0.72) eV, and (2.95) eV, respectively.

The refractive index n(0) and the high-frequency dielectric [50] are found to be the same (4.2) and (17.66).

Conclusions

In summary, sol-gel ZnO thin films were spin-coated onto glass substrates at a temperature of 6500C before being dyed with (P-Naphtholbenzenin()). We discovered a difference in grain size between ZnO pure (92nm) and ZnO: dye using the dip method (144nm). Despite the fact that the optical constants were determined using a UV-VIS spectrophotometer. The energy band distance Eg, as well as the oscillator parameters E0, Ed, and Eg, were measured and found to be (0.66, 0.72, 2.95) eV, indicating that the variations are due to the dye addition to ZnO.

References

[1]- Qiang Zhang, Shengwen Hou and Chaoyang Li," Titanium Dioxide –Coated Zinc Oxide Nanorods as an Efficient Photo electrode in Dye- Sensitized Solar Cells", 2020.

[2]- Gopalan, S.-A.; Gopalan, A.-I.; Vinu, A.; Lee, K.-P.; Kang, S.-W. Solar Energy Materials and Solar Cells A new optical-electrical integrated bu _ er layer design based on gold nanoparticles tethered thiol containing sulfonated polyaniline towards enhancement of solar cell performance. Sol. Energy Mater. Sol. Cells **2018**,174, 112–123.

[3]- Nandakumar, D.K.; Vaghasiya, J.V.; Yang, L.; Zhang, Y.; Tan, S.C. A solar cell that breathes in moisture for energy generation. Nano Energy **2020**, 68, 104263.

[4]- Nandakumar, D.K.; Ravi, S.K.; Zhang, Y.; Guo, N.; Zhang, C.; Tan, S.C. A super hygroscopic hydrogel for harnessing ambient humidity for energy conservation and harvesting. Energy Environ. Sci. **2018**, 11, 2179–2187.

[5]-. Kolodziejczak-Radzimska, A.; Jesionowski, T. Zinc oxide-from synthesis to application: A review. Materials (Basel) **2014**, 7, 2833–2881.

[6] . Lee, J.-C.; Gopalan, A.-I.; Saianand, G.; Lee, K.-P.; Kim, W.-J. Manganese and graphene included titanium dioxide composite nanowires: Fabrication, characterization and enhanced photocatalytic activities.Nanomaterials **2020**, 10, 456.

[7]- Tiwana, P.; Docampo, P.; Johnston, M.B.; Snaith, H.J.; Herz, L.M. Electro mobility and injection dynamics in mesoporous ZnO, SnO2, and TiO2 films used in dye-sensitized solar cells. ACS Nano. **2011**, 5, 5158–5166. [CrossRef

[8]- Vittal, R.; Ho, K.-C. Zinc oxide based dye-sensitized solar cells: A review. Renew. Sustain. Energy Rev. **2017**,70, 920–935.

[9]- Lu, L.; Li, R.; Fan, K.; Peng, T. E_ects of annealing conditions on the photoelectrochemical properties of dye-sensitized solar cells made with ZnO nanoparticles. Sol. Energy. **2010**, 84, 844–853.

[10]- Ambade, S.B.; Mane, R.S.; Ghule, A.V.; Takwale, M.G.; Abhyankar, A.; Cho, B.W.; Han, S.H. Contact angle measurement: A preliminary diagnostic method for evaluating the performance of ZnO platelet-based dye-sensitized solar cells. Scr. Mater. **2009**, 61, 12–15.

[11]- Yan, F.; Huang, L.; Zheng, J.; Huang, J.; Lin, Z.; Huang, F.; Wei, M. E_ect of surface etching on the e_ciency of ZnO-based dye-sensitized solar cells. Langmuir. **2010**, 26, 7153–7156.

[12]- Horiuchi, H.; Katoh, R.; Hara, K.; Yanagida, M.; Murata, S.; Arakawa, H.; Tachiya, M. Electron injection e_ciency from excited N3 into nanocrystalline ZnO films: E_ect of (N3-Zn2+) aggregate formation. J. Phys. Chem. B. **2003**, 107, 2570–2574.

[13]- Law, M.; Greene, L.E.; Radenovic, A.; Kuykendall, T.; Liphardt, J.; Yang, P ZnO-Al2O3 and ZnO-TiO2 core-shell nanowire dye-sensitized solar cells. J.Phys. Chem. B. **2006**, 110, 22652–22663.

[14]- Sabu, U.; Tripathi, N.; Logesh, G.; Rashad, M.; Joy, M.; Balasubramanian, M. Development of biomorphic C-ZnO with in situ formation of ZnS using eggshell membrane as bio-template. Ceram. Int. **2020**, 46, 22869–22875.

[15]- Camaratta, R.; Orozco-Messana, J.; Pérez Bergmann, C. Synthesis of ZnO through biomimetization of eggshell membranes using di_erent precursors and its characterization. Ceram. Int. **2015**, 41, 14826–14833.

[16]- Ian, Y.; Bu, Y. Improving the performance of dye-sensitized solar cells by incoporating a novel ZnO:Al charge injection layer. Optik **2020**, 205, 164242.

[17]- Prochowicz, D.; Mahdi, M.; Małgorzata, T.; Wolska-Pietkiewicz, M.J.; Trivedi, S.; Kumar, M.; Zakeeruddin, S.M.; Lewi´nski, J.; Graetzel, M.; Yadav, P. Suppressing recombination in perovskite solar cells via surface engineering of TiO2 ETL. Solar Energy **2020**, 197, 50–57.

[18]- Seow, Z.L.S.; Wong, A.S.W.; Thavasi, V.; Jose, R.; Ramakrishna, S.; Ho, G.W. Controlled synthesis and application of ZnO nanoparticles, nanorods and nanospheres in dye-sensitized solar cells. Nanotechnology **2008**, 20, 045604.

[19]- Nakade, S.; Saito, Y.; Kubo, W.; Kitamura, T.; Wada, Y.; Yanagida, S. Influence of TiO2 Nanoparticle Size on Electron Diffusion and Recombination in Dye-Sensitized TiO2 Solar Cells. J. Phys. Chem. B **2003**, 107, 8607–8611.

[20]- Theopolina Amakali, , Likius. S. Daniel 1 , Veikko Uahengo , Nelson Y. Dzade, and Nora H. de Leeuw "Structural and Optical Properties of ZnO Thin Films Prepared by Molecular Precursor and Sol–Gel Methods". Crystals **2020**,10, 132.

[2 1]- Mahdhi, H.; Djessas, K.; Ben Ayadi, Z. Synthesis and characteristics of Ca-doped ZnO thin films by rf magnetron sputtering at low temperature. Mater. Lett. **2018**, 214, 10–14.

[22]- Look, D.C. Mobility vs thickness in n + - ZnO films: E_ects of substrates and bu_er layers. Mater. Sci. Semicond. Process. **2017**, 69, 2–8.

[23]- Husna, J.; Aliyu, M.M.; Islam, M.A.; Chelvanathan, P.; Hamzah, N.R.; Hossain, M.S.; Karim, M.; Amin, N. Influence of annealing temperature on the properties of ZnO thin films grown by sputtering. Energy Procedia **2012**, 25,55–61.

[24]- Znaidi, L. Sol–gel-deposited ZnO thin films: A review. Mater. Sci. Eng. B **2010**, 174, 18–30.

[25]- Bahadur, H.; Srivastava, A.K.; Sharma, R.K.; Chandra, S. Morphologies of sol–gel derived thin films of ZnO using di_erent

precursor materials and their nanostructures. Nanoscale Res. Lett. **2007**, 2, 469–475.
[26]- Li, H.; Wang, J.; Liu, H.; Zhang, H.; Li, X. Zinc oxide films prepared by sol–gel method. J. Cryst. Growth **2005**, 275, e943–e946.
[27]- Khan, Z.R.; Khan, M.S.; Zulfequar, M.; Khan, M.S. Optical and structuralproperties of ZnO thin films Fabricated by Sol-Gel Method. Mater. Sci. Appl. **2011**, 2, 340–345.
[28]- Kim, K. Journal of the Korean Physical Society, Vol. 55, No. 1 (2009) 140.
[29]- Aldrish, fine chem.(1986-1987).
[30]- Cullity,B.D, Stock, S.R, Elements of X-Ray Diffraction , 3nd Ed., Prentice Hall, New York,(2001).
[31]- V.Pamuckchieva, A.Szekeres, Optical Mater. 30, 1088(2008).
[32]- Yakuphanoglu, F.; ¸Sekerci, M.; Ozturk, O.F. The determination of the optical constants of Cu(ii) compound having 1-chloro-2,3-o-cyclohexylidinepropane thin film. Opt. Commun. **2004**, 239, 275–280. [CrossRef]
[33]- Yakuphanoglu, F.; Arslan, M. Determination of thermo-optic coe_cient, refractive index, optical dispersion and group velocity parameters of an organic thin film. Phys. B Condens. Matter **2007**, 393, 304–309.
[34]- Brza, M.A.; Aziz, S.B.; Anuar, H.; Al Hazza, M.H.F. From green remediation to polymer hybrid fabrication with improved optical band gaps. Int. J. Mol. Sci. **2019**, 20, 3910.
[35]- Soylu, M.; Al-Ghamdi, A.A.; Yakuphanoglu, F. Transparent CdO/n-GaN(0001) heterojunction for optoelectronic applications. J. Phys. Chem. Solids **2015**, 85, 26–33.
[36]- Aziz, S.B.; Hussein, S.; Hussein, A.M.; Saeed, S.R. Optical Characteristics of Polystyrene Based Solid Polymer Composites: E_ect of Metallic Copper Powder. Int. J. Met. **2013**, 2013, 123657. [CrossRef]
[37]- S.Bhaskar, S.B.Majumder, M.Jain, P.S.Dobal, R.S.Katiyar, Material Science and Engineering B87 (2),178-190(2001).
[38]- R.Swanepoel, Journal of Physics E-Scientific Instuments 16,1214(1983).
[39]- Gao, X.; Du, Y.; Meng, X. Cupric oxide film with a record hole mobility of 48.44 cm2/Vs via direct-current reactive magnetron sputtering for perovskite solar cell application. Sol. Energy **2019**, 191, 205–209. [CrossRef]
[40]- Yakuphanoglu, F.; ¸Sekerci, M.; Ozturk, O.F. The determination of the optical constants of Cu(ii) compound having 1-chloro-2,3-o-cyclohexylidinepropane thin film. Opt. Commun. **2004**, 239, 275–280. [CrossRef]
[41]- Ahmed, N.M.; Sauli, Z.; Hashim, U.; Al-douri, Y. Investigation of the absorption coe_cient, refractive index, energy band gap, and film thickness for Al0.11Ga0.89N, Al0.03Ga0.97N, and GaN by optical transmission method. J. Nanoelectron. Mater. **2009**, 2, 189–195.
[42]. Baishya, U.; Sarkar, D. Structural and optical properties of zinc sulphide- polyvinyl alcohol (ZnS-PVA) nanocomposite thin films: E_ect of Zn source concentration. Bull. Mater. Sci. **2011**, 34, 1285–1288. [CrossRef]
[43]- Mansour, S.A.; Yakuphanoglu, F. Electrical-optical properties of nanofiber ZnO film grown by sol gel method and fabrication of ZnO/p-Si heterojunction. Solid State Sci. **2012**, 14, 121–126. [CrossRef]
[44]- Aziz, S.B.; Rasheed, M.A.; Ahmed, H.M. Synthesis of Polymer Nanocomposites Based on [Methyl Cellulose](1-x):(CuS)x (0.02 M _ x _ 0.08 M) with Desired Optical Band Gaps. Polymers **2017**, 9, 194. [CrossRef PubMed]
[45]- Aziz, S.B.; Mamand, S.M.; Saed, S.R.; Abdullah, R.M.; Hussein, S.A. New Method for the Development of Plasmonic Metal-Semiconductor Interface Layer: Polymer Composites with Reduced Energy Band Gap. J. Nanomater. **2017**, 2017,1–9. [CrossRef]
[46]- Meftah, A.M.; Gharibshahi, E.; Soltani, N.; Mat Yunus, W.M.; Saion, E. Structural, optical and electrical properties of PVA/PANI/Nickel nanocomposites synthesized by gamma radiolytic method. Polymers 2014, 6,2435–2450. [CrossRef]
[47]- Balestrieri, M. Transparent Conductive Oxides with Photon Converting Properties in View of Photovoltaic Applications: The Cases of Rare Earth-Doped Zinc Oxide and Cerium Oxide. 2015. Available online: https://tel.archives-ouvertes.fr/tel-01132180 (accessed on 29 July 2020).
[48]- Aziz, S.B.; Rasheed, M.A.; Abidin, Z.H.Z. Optical and Electrical Characteristics of Silver Ion Conducting Nanocomposite Solid Polymer

Electrolytes Based on Chitosan. J. Electron. Mater. **2017**, 46, 6119–6130. [CrossRef
[49]- S.Bhaskar, S.B.Majumder, M.Jain, P.S.Dobal, R.S.Katiyar, Material Science and Engineering B87 (2),178-190(2001).
[50]- H.S.Soliman, D.A.AbdelHady, K.F.AbdelRahman, S.B.Youssef, A.A.El-Shzly, Physics A; Statistial and Theoretial physics 216(1-2),7784(1995).